Structural modification of Al–Si eutectic alloy by Sr and its effect on tensile and fracture characteristics

N. FAT-HALLA
Mechanical Department, Faculty of Engineering, Al Azhar University, Cairo, Egypt

Modification of the commercial A-S13 alloy and high purity Al–Si eutectic alloy has been successfully achieved using Al–5 Sr master alloy. The refined structure showed more fine and uniformly distributed eutectic silicon in the high purity alloy. The incidence of Al-dendrites due to modification was related to the movement of the eutectic point to the higher-silicon side. The chill-cast alloys showed better refined structure and higher mechanical properties in comparison with the sand-cast alloys. The modified chill-cast alloy exhibited the best mechanical properties. The ultimate tensile strength of which reached 280 MPa and the elongation was 9.2%. The fracture patterns changed from well faceted brittle appearance to smooth silky and dimple-like for the normal and modified alloys respectively. This reflects the change from brittle to ductile behaviour after modification. A model for the fracture mechanism was proposed to explain the observed higher ductility for the modified alloy.

1. Introduction

The commercial Al–Si eutectic alloy is of great industrial importance. Its typical uses are: miscellaneous thin walled and intricately designed castings [1]. The discovery of modification of Al–Si alloys by Pacz [2] has undoubtedly explored better and extensive uses of the alloy. Additionally, it attracted the attention of many investigators to further develop these alloys. However, since Chalmers [3, 4] has reviewed the types and mechanisms of formation of some eutectic systems focusing on the Al–Si alloy, very rare reports have been published in this area of research [5–10]. For Al–Si eutectic alloy, the information about the tensile properties [1, 4–6, 8–11] and fracture [4, 9, 11] are scattered and incomplete.

The present author has recently reported about the mechanical properties and fracture of some hypoeutectic alloys [12–15]. However, gaps in this area have not been completely covered. The goal of the present investigation is to study the structural changes due to modification by Al–5 Sr master alloy for Al–Si eutectic alloy. The effect of microstructure on the tensile properties and fracture characteristics is investigated.

2. Experimental procedure

Two eutectic Al–Si alloys have been used in the present investigation being the commercial A-S13 and high purity Al–12.7% Si. The chemical composition of the A-S13 alloy is given in Table I.

It was found that when accurately balanced small pieces of Al–5 Sr master alloy were added to the molten metal (0.02% Sr in the eutectic alloy) and it was then manually stirred at the beginning of the melt and the melt was held for 0.3 ksec at the superheating temperature of about 1000 K prior to casting, the results were satisfactory and the alloy had a modified structure. For the sake of comparison sand- and chill-casting of the nonmodified and modified alloys have been made.

Cylindrical tensile test specimens were machined to a gauge diameter of 5 mm and gauge length of 10 mm. The tensile tests have been carried out at room temperature of 300 K and strain rate of $10^{-3}\,sec^{-1}$. In the present investigation the well known techniques of optical metallography have been used [12, 16]. Fractographic study has been carried out using the SEM following the standard techniques [15, 17].

3. Results and discussion

Figure 1 shows the microstructure of the high purity sand-cast eutectic alloy (similar structure was observed for the A-S13 alloy under the same conditions). The photograph shows discontinuous microstructure in which the Si-phase is dispersed in the Al-matrix as discrete particles (needle-like morphology). It was reported however, that what appears as a needle in a two-dimensional section must be a sheet or flake [4, 11].

Chill casting of the eutectic Al–Si alloy, generally, shows refinement of the eutectic. Figure 2 delineates the microstructure of the A-S13 alloy as chill cast. The shape of the Si particles is the same as in slowly cooled alloys but are scaled down to very much smaller dimensions. The refinement of the structure is accompanied by the appearance of primary Al-dendrites, which has led to the suggestion that the eutectic composition has been moved to higher Si contents as

0022-2461/89 $03.00 + .12

TABLE I Chemical composition of the commercial alloy A-S13

Element	Mass (%)	Element	Mass (%)
Fe	00.40	Zn	00.12
Si	11.70	Ti	00.10
Cu	00.05	Co	00.16
Mg	00.08	Pb	00.08
Mn	00.20	Sn	00.05
Ni	00.05	Al	Balance

a result of the rapid cooling. Rapid cooling is also known to produce a sharp decrease in the temperature of the eutectic arrest [3, 4]. The present result is in consistence with the appearance of the coupled region during rapid solidification of Al–Si eutectic alloy, which shows, a movement of the eutectic composition with undercooling [3]. On the other hand, the fine lamellar structure obtained under the rapid cooling conditions (chill-casting) exhibits microstructures and properties which are not only better than those of slowly cooled alloys but also comparable to the modified eutectic alloys. It is now to be mentioned that the Si-content in the A-S13 alloy (see Table I) is slightly in the hypoeutectic side. Therefore, the incidence of the Al-dendrites in Fig. 2 is due to both reasons; (i) the coupled region phenomenon [3], and (ii) the Si content in the A-S13 alloy (see the Al–Si phase diagram [13, 16]).

After addition of 0.02% Sr to the molten metal of the A-S13 and high purity eutectic alloys, as mentioned in detail in the procedure, the resulting microstructure is shown in Fig. 3a and b respectively. The general features of the two photographs are; the occurrence of primary Al-dendrites and the refinement of the eutectic matrix. It is now pertinent to discuss the phenomenon of the occurrence of primary Al-dendrites. When the alloy is rapidly chilled, the melt is supercooled and the first formed Al-dendrites can grow very quickly into the liquid before the Si-phase is nucleated. We would therefore, expect more primary Al-phase in chill-cast alloys than in slowly cooled ones [3–6, 9]. Moreover, for the Sr-modified eutectic alloy which is assumed to solidify quite naturally with a finer microstructure than the binary alloy, a ternary eutectic (Sr and Al–Si compound) is formed.

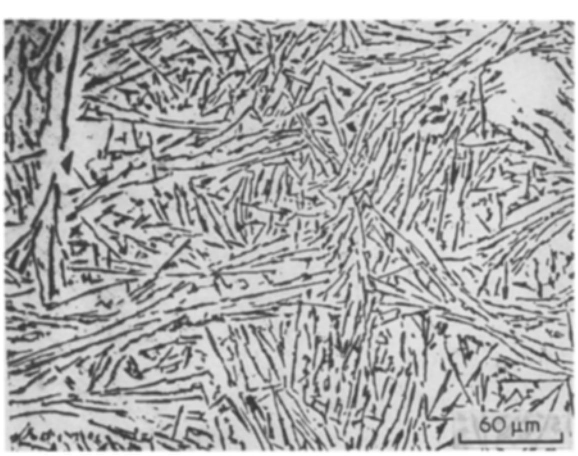

Figure 1 The microstructure of high purity sand-cast eutectic alloy. 7.6 cm wide × 5.8 cm deep.

Figure 2 The microstructure of A-S13 alloy as chill-cast. 8.2 cm wide × 6.2 cm deep.

The equilibrium freezing point of the ternary eutectic is supposed to be 10–15 K [3] below the binary eutectic temperature, and at the same time the eutectic composition is assumed to be displaced to higher Si-contents to account for the presence of primary Al-dendrites which appear in the present modified alloys.

On the other hand, two main differences do exist between the photos in Fig. 3a and b or the modified A-S13 and high purity eutectic Al–Si alloys respectively. First; the volume fraction of the primary Al-phase in the former is about 20% which reflects both the movement of the eutectic point and also the result of the original slight deviation from the eutectic point (12.5 mass % Si) to hypoeutectic side (see Table I). While the latter shows primary Al-dendrites of about 13.5% (volume fraction was measured by the point counting technique [16]). This latter ratio reflects the movement of the eutectic point to the higher silicon side by about 1% Si. These results are in agreement with those reported previously [3–6, 9]. Secondly, the refined eutectic of the high purity alloy observed in Fig. 3b is finer and more uniformly distributed than that of the A-S13 observed on Fig. 3a. This may stem from the difference in purity of the two alloys or due to the difference in the silicon content in both alloys.

The results of the tensile properties for both the modified and nonmodified A-S13 and high purity eutectic alloys cast in different moulds are shown in Table II.

It can be noted from Table II that modification, in general, while moderately increased the strength of the different alloys it drastically increased the percentage elongation. The elongation of the modified high purity eutectic alloy is in general better than that of the modified commercial A-S13 alloy. This slight increase in elongation is believed to be related to the difference between the modified microstructures of Figs 3a and b. The finer and more uniformly distributed eutectic structure of Fig. 3b resulted in the better elongation observed in Table II.

Pacz [2] observed that the fracture surfaces of non-modified cast Al–Si alloys had very coarse, dark and crystalline features and that after modification by sodium the features turns to fine grained light and

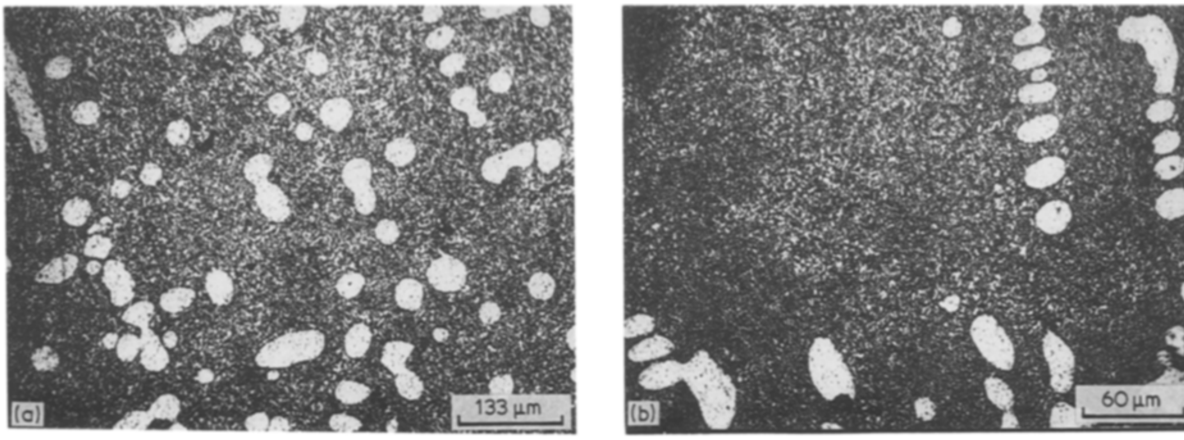

Figure 3 (a) Modified commercial A-S13 alloy microstructure, (b) modified high purity Al–Si eutectic alloy microstructure. (a) 7.73 cm wide × 5.9 cm deep, (b) 7.8 cm wide × 5.95 cm deep.

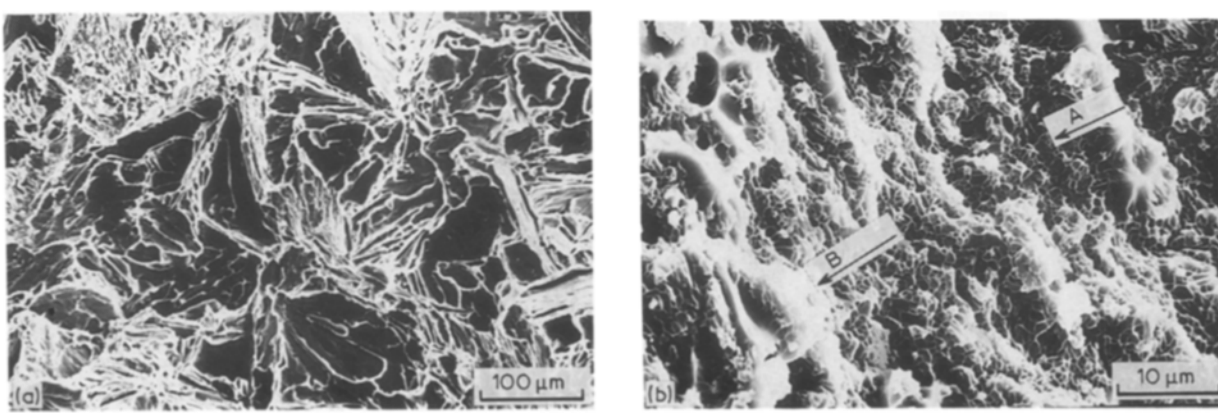

Figure 4 (a) The fracture surface of the nonmodified A-S13 alloy (sand-cast), (b) same as in (a) but chill-cast. (a) 7.9 cm wide × 5.5 cm deep, (b) 8.1 cm wide × 5.3 cm deep.

dense appearance. However, very little information has been reported after that about the fracture of Al–Si eutectic alloy [4, 9, 11]. To further develop the mechanical properties of this alloy it is better to understand its fracture phenomena.

Figure 4a shows a photomicrograph of the fracture surface of the nonmodified A-S13 alloy (sand-cast) as observed by the SEM. It delineates well faceted brittle appearance which resembles the appearance of the Si-particles (cf. Fig. 1). This photo explains the low ductility of the alloy (2.2%) as was indicated in Table II. Figure 4b shows the same nonmodified eutectic alloy but as chill-cast. Faceted regions can also be observed as indicated by arrow "A" but on a much smaller scale as compared with Fig. 4a. Additionally, smooth regions, indicated by arrow "B", can be observed (it might be Al-phase). Figure 4b therefore, gives some indications of better ductility compared to Fig. 4a. This result is in consistence with the elongation results given in Table II.

Figures 5a and b show the features of the fracture surface of the modified A-S13 alloy (sand-cast) at intermediate and high magnification. These photos delineate two main features, Fig. 5a, being (i) smooth silky areas (Al-phase), and (ii) semiequiaxed dimples Fig. 5b shows at a higher magnification the semi-dimple pattern (indicated by arrow "A") and smooth silky regions (indicated by arrow "B"), which suggests

TABLE II Tensile properties of the modified and nonmodified eutectic alloys

	Mould type	0.2% Proof stress (MPa)	UTS (MPa)	Elongation (%)
Nonmodified A-S13	Sand	60	130	2.2
	Metal	70	160	4.3
Modified A-S13	Sand	100	180	8.0
	Metal	106	200	8.7
Nonmodified (high purity)	Sand	100	153	3.0
(12.7% Si)	Metal	150	254	5.5
Modified (high purity)	Sand	104	180	8.3
(12.7% Si)	Metal	147	280	9.2

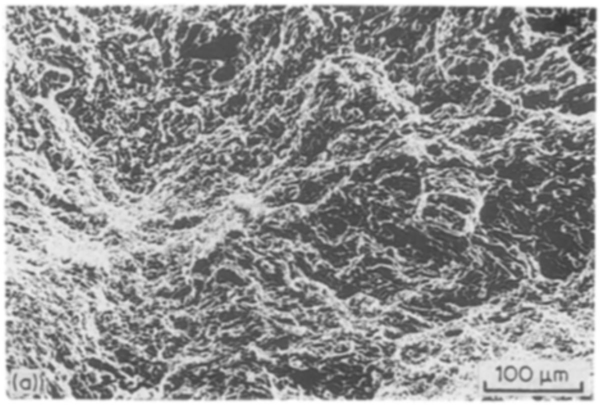

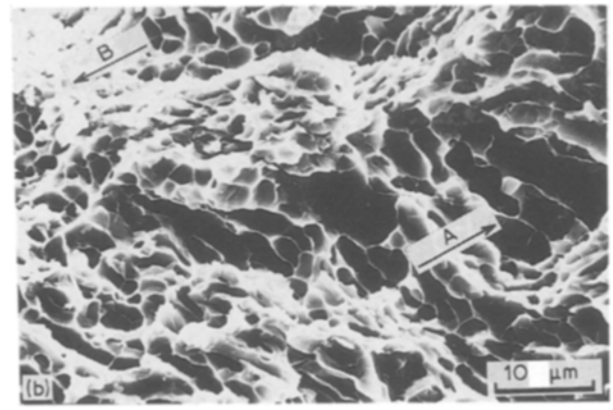

Figure 5 (a) Features of the fracture surface of the modified A-S13 alloy (sand-cast), (b) same as in (a) but at higher magnification. (a) 8 cm wide × 5.3 cm deep, (b) 8.1 cm wide × 5.6 cm deep.

that fracture has occurred largely through the ductile Al-matrix.

4. Mechanism of fracture of modified Al–Si eutectic alloy

When soft and hard phases coexist in a material such as the case in eutectic Al–Si alloy, many factors do affect the deformation and fracture characteristics. These factors include the size, shape, number and distribution of the second phase particles, the strength, ductility and strain-hardening behaviour of the matrix and second phase, the crystallographic orientation, relationship between the phases and the interfacial bonding between the phases. The problem of fracture in a two phase alloy has been previously discussed [18]. However, in the present investigation the need for an explanation of the increased ductility of the modified alloy arises.

In the proposed model (Fig. 6) for the fracture mechanism it will be assumed that hard silicon spheres are uniformly distributed in a soft Al-matrix representing an idealized modified Al–Si eutectic alloy microstructure. The fracture path will continue to propagate across the soft-Al-matrix circumventing the hard silicon-spheres. The fracture surface, therefore, will exhibit smooth silky appearance (cf. Fig. 5b). Whether the fracture path propagates intergranularly along the aluminium grain boundaries or transgranularly across the aluminium grains is a moot point and needs further study. This model is in consistence with the previous publications [4, 9, 11] which suggested that fine, rounded silicon particles would not transmit cracks through the material easily as would coarse flakes of Si and that the modified material could be regarded as a dispersion-hardened Al-solid solution.

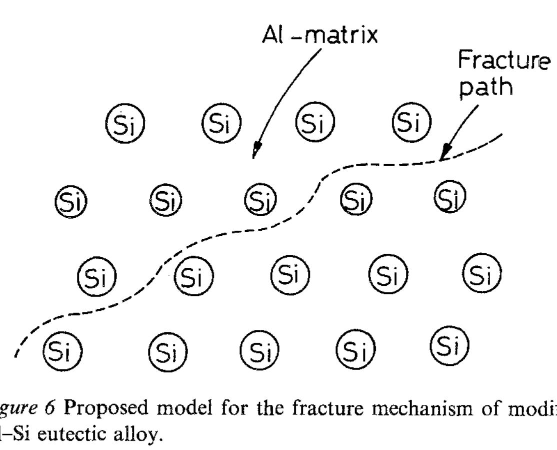

Figure 6 Proposed model for the fracture mechanism of modified Al–Si eutectic alloy.

5. Conclusions

1. Commercial A-S13 alloy and high purity Al–Si eutectic alloy have been successfully modified using Al–5 Sr master alloy (0.02% Sr).

2. High purity eutectic showed better modified microstructure (more finely and uniformly distributed eutectic silicon).

3. The incidence of Al-dendrites in the microstructure of the modified Al–Si eutectic was attributed to the movement of the eutectic point due to modification.

4. Faster cooling rate (chill-casting) resulted in refine eutectic and better mechanical properties in comparison with slow cooling rate (sand-casting).

5. Modified chill-cast Al–Si eutectic alloy exhibited best mechanical properties. Tensile strength reached 280 MPa at an elongation of 9.2%.

6. Fractography of the sand-cast eutectic revealed well faceted brittle appearance which resembles the appearance of the Si-particles.

7. Fracture surfaces of the modified Al–Si eutectic alloy revealed smooth silky areas and semi-dimple pattern reflecting the tendency towards ductile rupture.

8. A model was proposed for the fracture mechanism of the modified Al–Si eutectic alloy.

References

1. T. LYMAN, "Metals Handbook" (The American Society for Metals, Ohio, 1948).
2. A. PACZ, USA Patent No. 1387900 (1920).
3. B. CHALMERS, "Progress in Materials Science", Vol. 12 (Pergamon Press, Oxford, 1965).
4. *Idem*, "Progress in Materials Science", Vol. 15 (Pergamon Press, Oxford, 1970).
5. J. CHARBONNIER, J. PERRIER and R. PORTALIER, *AFS Int. Cast Metals J.* **3** (1978) 17.
6. P. DAVAMI and M. GHAFELEHBASHI, *British Foundryman* **72** (1979) 4.
7. G. NAGEL and R. PORTALIER, *AFS Int. Cast Metals J.* **5** (1980) 2.
8. J. PAUL, H. EXNER and D. MÜLLER-SCHWELLING, *Z. Metallkde* **73** (1982) 50.

9. M. M. HAQUE, *Metals Forum* **6** (1983) 54.
10. M. M. HAQUE, G. H. BENNETT and V. KONDIC, *Foundry Trade J.* (1983) 387.
11. L. F. MONDOLFO, "Aluminium Alloys: Structure and Properties" (Butterworths, London, 1976).
12. N. FAT-HALLA, Current Advances in Mechanical Design and Production, 3rd Cairo University MDP Int. Conference, Cairo, December 28–30, 1985 (Pergamon Press, Oxford, 1985) pp. 239–246.
13. N. FAT-HALLA, *J. Mater. Sci.* **22** (1987) 1013.
14. N. FAT-HALLA, P. SECORDEL and M. SUERY, *J. Mater. Sci.* **23** (1988) 2419–2423.
15. *Idem*, 5th International Conference on Mechanical Behaviour of Materials, Beijin, China, 3–6 June, 1987 (Pergamon Press, Oxford, 1987) pp. 1419–1426.
16. ASM Metals Handbook, "Metallography, Structures and Phase-Diagrams", Vol. 8 (ASM, Ohio, 1973).
17. ASM Metals Handbook, "Fractography and Atlas of Fracture", 8th Edn (ASM, Ohio, 1974).
18. N. FAT-HALLA, T. TAKASUGI and O. IZUMI, *J. Mater. Sci.* **13** (1978) 2462.

Received 25 April
and accepted 5 September 1988